Label-Free Quantification of Anticancer Drug Imatinib in Human Plasma with Surface Enhanced Raman Spectroscopy

Stefano Fornasaro,[*,†] Alois Bonifacio,[†] Elena Marangon,[‡] Mauro Buzzo,[‡] Giuseppe Toffoli,[‡] Tomas Rindzevicius,[§] Michael Stenbæk Schmidt,[§] and Valter Sergo[†,∞]

[†]Department of Engineering and Architecture, University of Trieste, Via Valerio 6A, 34127 Trieste, Italy

[‡]Experimental and Clinical Pharmacology Division, CRO Aviano−National Cancer Institute, Aviano, Italy

[§]Department of Micro- and Nanotechnology, DNRF and Villum Fonden Center for Intelligent Drug Delivery and Sensing Using Microcontainers and Nanomechanics, IDUN, Ørsteds Plads, 2800 Kongens Lyngby, Denmark

[∞]Faculty of Health Sciences, University of Macau, Macau SAR, China

Supporting Information

ABSTRACT: Therapeutic drug monitoring (TDM) for anticancer drug imatinib has been suggested as the best way to improve the treatment response and minimize the risk of adverse reactions in chronic myelogenous leukemia (CML) and gastrointestinal stromal tumor (GIST) patients. TDM of oncology treatments with standard analytical methods, such as liquid chromatography−tandem mass spectrometry (LC−MS/MS) is, however, complex and demanding. This paper proposes a new method for quantitation of imatinib in human plasma, based on surface enhanced raman spectroscopy (SERS) and multivariate calibration using partial least-squares regression (PLSR). The best PLSR model was obtained with three latent variables in the range from 123 to 5000 ng/mL of imatinib, providing a standard error of prediction (SEP) of 510 ng/mL. The method was validated in accordance with international guidelines, through the estimate of figures of merit, such as precision, accuracy, systematic error, analytical sensitivity, limits of detection, and quantitation. Moreover, the feasibility and clinical utility of this approach have also been verified using real plasma samples taken from deidentified patients. The results were in good agreement with a clinically validated LC−MS/MS method. The new SERS method presented in this preliminary work showed simplicity, short analysis time, good sensitivity, and could be considered a promising platform for TDM of imatinib treatment in a point-of-care setting.

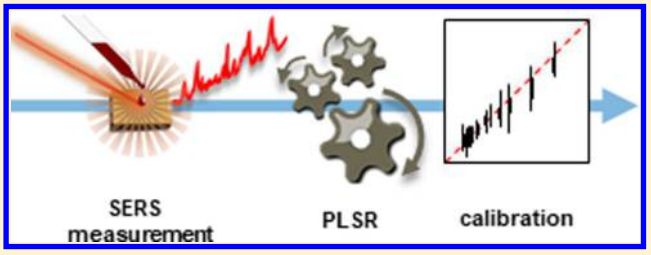

Imatinib (IMT) is a 2-phenylaminopyrimidine compound (Figure 1) that represents the first in a class of oral targeted anticancer drugs (tyrosine kinase inhibitors, TKIs) currently approved by the European Medicines Agency (EMA) and by the U.S. Food and Drug Administration (FDA) for the treatment of different cancers, such as chronic myelogenous leukemia (CML) and gastrointestinal stromal tumor (GIST). TKIs are characterized by a unique mechanism of action and are highly specific for cellular biological pathways involved in the angiogenesis and in tumoral proliferation. The therapeutic results of treatment with TKIs can be affected by factors such as large pharmacokinetic variability and individual patient variability in absorption, distribution, and metabolism. This large variability is possibly affected by factors such as food−drug interaction and drug−drug interaction; moreover, TKIs are highly but differently bound to circulating proteins in plasma such as α-1-acid glicoprotein [AGP] and albumin and, consequently, the mean unbound fraction of IMT presents a high interindividual variability.[1−4] For IMT, a concentration-effect relationship has been observed in both CML[5] and GIST[6] patients. Toxicity increases at high plasma levels whereas an impaired efficiency, leading to subsequent therapeutic failure, was associated with low plasma levels. While there is no clear

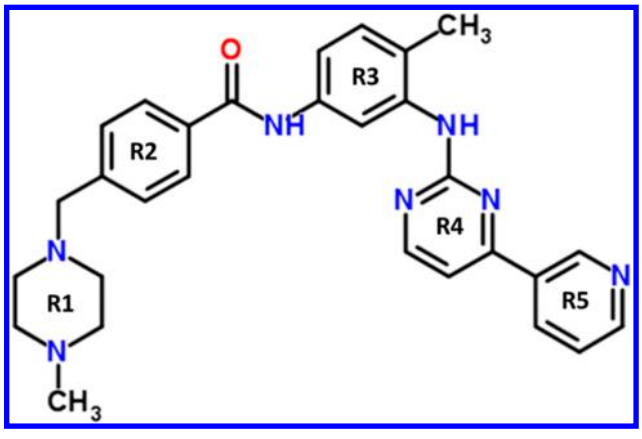

Figure 1. Chemical structure of imatinib.

Accepted: September 28, 2018

pharmacokinetic cutoff related to intolerable toxicities, a lower limit for IMT trough plasma concentrations, C_{trough}, has been proposed. An IMT plasma C_{trough} of 1002 ng/mL or 1100 ng/mL as the pharmacokinetic target is currently recommended for CML or GIST patients, respectively.[7] Moreover, the oral targeted drugs are extremely expensive, thus an accurate dosage in function of benefit/toxicity ratio might represent also an economic benefit.[8] Taking all these factors into consideration, therapeutic drug monitoring (TDM) should probably be the best way to reliably control the plasma concentrations of IMT in GML and GIST patients, improving the treatment response and minimizing the risk of adverse reactions. However, if performed, TDM is carried out in centralized laboratories and core facilities within specific clinical research programs, still far from the routine practice. For instance, current attempts to measure IMT in biofluids employ techniques such as liquid chromatography−tandem mass spectrometry (LC−MS/MS),[9] high-performance liquid chromatography coupled to ultraviolet (HPLC−UV).[10,11] Though highly sensitive and specific, such techniques are expensive, time-consuming, and need qualified and trained personnel. With this regard, the development of a new generation of nanotechnological analytical tools and their clinical applications in medicine has increasingly gained value.[12] Surface enhanced Raman spectroscopy (SERS) has lately drawn growing attention as a tool to measure low concentrations of compounds in body fluids, providing a fast and relatively cheap alternative analytical platform for TDM.[13] Rath et al. reported a proof of concept for the detection, but not for quantification, of IMT in human plasma at concentration of 1.7 μM (839 ng/mL) and above with SERS.[14] However, SERS approaches quantifying IMT directly in plasma or other complex biofluids have not been reported yet. In this work, we present a spectroscopy-based point-of-care approach for a fast and inexpensive determination of IMT, thus offering to medical doctors an affordable protocol for dosing IMT.

EXPERIMENTAL SECTION

Chemicals. Imatinib European Pharmacopoeia (EP) Reference Standard and potassium mesylate were purchased from Sigma-Aldrich (St. Louis, MO). Imatinib hydrochloride (≥98% purity) was purchased from Cliniscience srl (RM, Italy). All solvents were at analytical grade and used without further purification. Milli-Q water was prepared with a Millipore apparatus. All reagents were handled according to their respective safety data sheet.

Samples Preparation. Stock solutions with a concentration of 1.0 mg/mL of IMT were prepared by dissolving the dry IMT powder in 100% methanol and were appropriately diluted with methanol for the preparation of standard working solutions with final concentrations ranging from 0 to 100 μg/mL. Human plasma/K_2-EDTA was provided by the transfusion unit of the National Cancer Institute (CRO, Aviano, Italy) from healthy volunteers. On the day of the analysis, aliquots of plasma were thawed on ice and alternatively spiked by 1:20 dilution of the pertinent standard working solution to maintain the same dilution factor (total added volume ≤10% of the biological sample volume), across all samples, in accordance with the recommendations on bioanalytical method validation.[15] The order of sample preparation was randomized to avoid bias. Samples for method validation were prepared at 11 concentrations (104, 207, 316, 420, 627, 1046, 1254, 1673, 2093, 3139, 4186 ng/mL) in accordance with observed clinical range of IMT C_{trough} levels (355−4400 ng/mL).[2] IMT is stable in blood and plasma for at least 96 h at room temperature.[11,16] All aliquots (57 μL plasma spiked with 3 μL IMT standard working solution) were placed into a 1.5 mL polypropylene microcentrifuge tubes along with 180 μL of 4:1 v/v MeOH/2% $ZnSO_4$ aqueous solution, to break down noncovalent drug−protein interactions and, at the same time, to induce protein precipitation. This mixture was then vortexed vigorously for 10−20 s and kept at 4 °C for 10 min to promote further protein precipitation and maximize the recovery of the strongly protein-bound IMT. The mixtures were then centrifuged at 13 200 rpm for 10 min at room temperature and the colorless supernatant (∼150 μL) was transferred to a 500 μL vial, for subsequent SERS analysis.

SERS Substrates and SERS Measurements. Nanostructured SERS substrates comprising of freestanding vertical silicon nanopillars coated with silver were provided by Silmeco (Copenhagen, Denmark) and used as received. Before preparation, the silver coated nanopillars are vertically oriented and highly packed (∼20 pillars/μm^2). After sample incubation and solvent evaporation, the high aspect ratio and thus flexible nanopillars lean toward each other, due to the surface tension during the drying process.[17] As the silver coated nanopillars lean toward each other, electromagnetic "hotspots" are formed due to the coupling effect of localized surface plasmon resonances (LSPRs) between adjacent nanostructures.[18] Substrates were incubated with IMT solutions for 15 min at room temperature in dark conditions to eliminate any photochemical effects. Subsequently, the substrates were rinsed with Milli-Q water to remove species with unspecific binding to the metal surface before being allowed to dry. Seven technical replicates were prepared for each concentration.

SERS Data Collection. SERS spectra were recorded in air at room temperature (22 ± 0.5 °C) with a portable i-Raman Plus integrated system (BWS465-785S, B&W Tek, Newark, DE). The instrument was equipped with a CleanLaze 785 nm laser, tuned to deliver 15 mW at the sample, on a spot of about 105 μm in diameter, through the BAC151B Raman Video Microsampling System mounting a 20× Olympus objective (working distance 8.8 mm, N.A. 0.25). Each 4 mm × 4 mm SERS substrate was put on a standard microscope slide (25 mm × 75 mm) that was fitted onto the microscope stage. Spectra were collected using a 10 s CCD exposure for 3 accumulations, in the Raman shift range 62−3202 cm^{-1}, with an average spectral resolution of 3.22 cm^{-1}. Wavenumber calibration was checked before each measurement session by collecting a spectrum from paracetamol as a standard reference. To compensate for intrasubstrate variability, three spectra were averaged for each substrate as the final spectrum for that specific sample. The spectral acquisition was performed with the BWSpec version 4.03_23_c (B&W Tek, Newark, DE) software. The BWSpec software allowed to collect a background signal (dark) before data acquisition and to subtract it from collected data.

Chemometrics SERS Data Processing. All data preprocessing and analysis were performed within the R software environment (version 3.4.3) for statistical computing and graphics, building on the packages *hyperSpec*,[19] *chemometrics*,[20] *EMSC*,[21] *pls*,[22] and *ggspectra*[23] on a commercially available workstation (Intel Core i7−4770, 4 cores 3.40 GHz, 32 GB DDR3-RAM). In-house developed R scripts were used for visualization and further processing. All spectra underwent a smoothing interpolation (*spc.loess*) onto an evenly spaced

wavenumber axis from 350 to 2000 cm^{-1} with data point spacing of 3 cm^{-1}. This decreases the number of variables, stabilizing the subsequent model. Extended Multiplicative Scatter Correction (EMSC), as implemented in the EMSC package,[21] was then used to remove offsets and baseline slopes, taking into account unspecific scattering contributions and variability within the spectral data set, and to effectively normalize the spectra in the entire spectral region. This kind of model-based preprocessing technique, takes the information registered in the spectra to simultaneously correct for additive (baseline) and multiplicative (normalization) effects, essentially by projecting each spectrum in the data set onto a reference spectrum.[24−26] In this study, the reference spectrum was established by considering the mean spectrum of 18 SERS spectra of plasma, independently recorded from healthy donors (9 men and 9 women). The effect of the complete preprocessing procedure can be seen in Figure S2. Multivariate calibration was performed using partial least-squares regression (PLSR)[27,28] by regressing the preprocessed (without scaling) spectra versus the theoretical values of the drug in spiked samples. PLSR describes a given response (dependent variable) as a function of a few latent variables (LVs). The LVs are derived from the original variables as linear combinations, which maximally capture the covariance between the independent variables (data matrix of intensity values) and the dependent variables (vector of analyte concentrations). More details on PLSR for multivariate calibration can be found in refs 27 and 28. The performance of the PLSR model was evaluated by a repeated double cross validation (rdCV) strategy, as proposed by Filzmoser and coworkers.[29] Briefly, a randomly chosen subset of data, the calibration set, was subjected to a k-fold cross validation loop, yielding a first suggestion for the optimum model complexity. Subsequently, a model for the entire calibration set is constructed and applied to the left out test data. The procedure described above is repeated several times, thus producing many test sets and then using the optimum number of PLS components determined from the inner loop to estimate the prediction error with error bounds. In this work; the number of repetitions was 100 (with different random sequences of the objects); the data set was split into four segments in the outer CV loop (test sets) and seven segments in the inner CV loop (optimal number of variables). The optimum number of PLS latent variables (LVs) was assessed based on a "*one-standard error*" method, (π = 1) as proposed by Hastie and Tibshirani.[29,30] The quality of PLSR model was assessed by standard error of prediction (SEP), which is defined as the standard deviation of the predicted errors (residuals) bias, defined as the arithmetic mean of the prediction errors, and the square of the correlation coefficient (R^2) between predicted and actual values. Due to the iterated nature of rdCV, the variability of optimum model complexity as well as the variability of test-set predicted errors with different data subsets are accessible.

Reference Method. The LC−MS/MS apparatus consisted in a Prominence XR HPLC (Shimadzu) coupled with an ESI triple quadrupole mass spectrometer API4000 QTrap (SCIEX). The analytes (imatinib and its main metabolite, *N*-desmethyl imatinib) were extracted from plasma samples thanks to a simple protein precipitation with methanol and they were separated in a 50 mm × 2.0 mm C18 analytical column Synergi Fusion RP (Phenomenex). Gradient elution was chosen to obtain a faster chromatographic separation and to address the poor cleanness of the samples. The electrospray source worked in positive ion mode and, for the quantification, the analyzer was set in selected reaction monitoring following the transitions 494.4 > 394.2 and 480.4 > 394.2 for imatinib and *N*-desmethyl imatinib, respectively. In order to minimize the matrix effect, a deuterium-labeled form of the analyte (imatinib-d8) was chosen as internal standard. Linearity (from 30 to 7500 ng/mL, covering the entire clinical range), recovery, selectivity, inter- and intraday precision and accuracy, stability, and reproducibility were assessed and the quantification method was validated according to the FDA and EMA guidelines.

Analytical Validation. Figures of merit (FOM) are concepts and terms used to describe the analytical performance of a particular measurement procedure. Unfortunately, literature in this area has been, and still is, confusing with respect to concepts, nomenclature, and methods. The approach employed here was based on recent recommendations by EURACHEM guide.[31] Thus, the following FOM were determined: limit of decision (CCα), limit of detection (CCβ), limit of quantitation (LOQ), sensitivity (SEN), analytical sensitivity (γ). Ten independent measurements of blank samples were used to estimate the experimental noise level. Full details are provided in the Supporting Information Supplementary Methods section. The generalization of the procedure to obtain such FOM with multivariate calibrations can be found in the literature.[32−35] Since the lack of standardization between different FOM described in the literature for multivariate methods leads to a rather confusing situation,[36] trueness and accuracy were also evaluated by comparing the results of the proposed method with those of a second standard procedure (HPLC−MS), already used in hospitals for TDM of drugs, for six real clinical samples (i.e., plasma of patients treated with IMT). For each sample, the difference between two measurements was calculated, and the Bland-Altman method[37] was used to compare the two analytical techniques.

RESULTS AND DISCUSSION

Optimization of SERS for Detection of Imatinib in Human Plasma. Initial studies used our previously optimized conditions for the production of SERS solid substrates on paper;[38,39] however, when using these substrates plasma samples spiked with clinically relevant concentrations of IMT did not contain any specific spectral features from the target drug. Two of the most critical problems in IMT plasma determination with SERS are (i) the sequestration into bulk solution of a relevant fraction of the drug (95% is bound mainly to alpha-glycoprotein and albumin),[1] and (ii) the competition with plasma constituents for the metal surface. Accordingly, we decided to use the silver SERS substrates from Silmeco (Figure 2), which proved to be more sensitive, and to reduce the plasma complexity at the metal surface by an efficient and fast deproteinization process. All the details about the SERS substrates can be found in literature.[40,41] Different protein precipitation protocols were thus examined to establish the optimum conditions providing the highest reproducibility and stability of the signal, yielding spectral features that could be assigned to IMT (Figure S1). According to these experiments, the combination of methanol with $ZnSO_4$ provided the most reproducible and information-rich SERS spectra, and, hence, this procedure was adopted throughout this study. The Zn^{2+} binds to proteins in the plasma, forming a

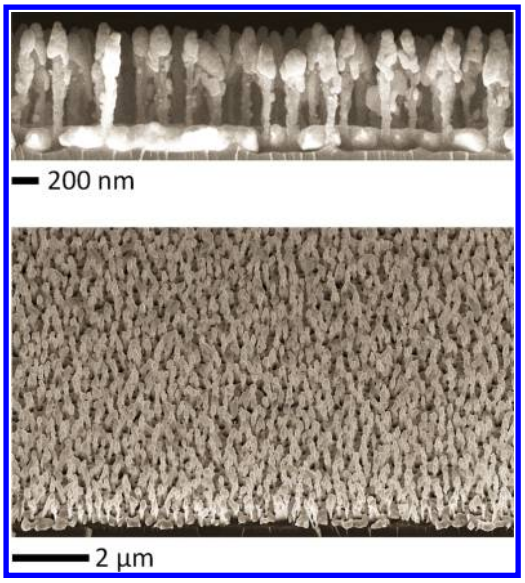

Figure 2. Scanning electron microscope image of the SERS substrate used. (Top) High magnification image taken at an angle of 90° to the surface. The silicon nanopillars are seen to be coated by a layer of silver which also covers the base of the substrate. (Bottom) Image taken at a 45° angle with respect to the surface. The macro uniformity of the nanopillars is clearly seen across the surface.

precipitate of insoluble metal-protein salt complexes. In addition, as Zn^{2+} binds to the amino acids, protons are displaced, thus decreasing the pH of the sample,[42] which, in turn, can decrease the Log *D* values of ionizable compounds and improve their solubility in methanol. The use of a protic solvent like methanol helps to improve the solubility of the drug boosting recovery of hydrophobic compounds.[43]

SERS Detection of Imatinib in Human Plasma. Figure 1 reports the IMT chemical structure. IMT consists of a pyridine ring (R5), an aminopyrimidine ring (R4), a methylbenzene ring (R3), a benzamide ring (R2), and a *N*-methylpiperazine ring (R1). Figure 2 shows the SERS spectrum of the IMT (6.36 μM) detected in plasma (B) compared with at the SERS spectrum of IMT in MeOH/Zn^{2+} solution (C). SERS spectrum of deproteinized plasma (A) and Raman spectrum of IMT powder (D) are reported for comparison. The average SERS spectrum of plasma after protein purification (A) is consistent with SERS spectra of filtered (deproteinized) plasma on various substrates previously reported in literature: a comparison of the spectra of plasma samples collected after deproteinization for this study with previous findings from our group[44] and from Premasiri et al.,[45] suggests that the protein components of plasma do not contribute to the main SERS spectral features: the most significant peaks at 485, 644, 716, and 1133 cm^{-1}, are mainly attributed to uric acid and hypoxanthine. As this paper is concerned with IMT detection in plasma, it is noteworthy that the SERS bands appearing at 988, 1032, 1307, and 1606 cm^{-1} in the spectrum of IMT in MeOH/Zn^{2+} solution (Figure 2C), can be easily distinguished also in the SERS spectra of IMT in plasma (Figure 2B); indeed the Raman and SERS bands observed for the IMT were consistent with those reported in literature.[14,46] In other words, after a deproteinization step, SERS can successfully detect IMT in plasma. Most likely, IMT bands are readily observed in deproteinized plasma because the concentration of "free", unbound IMT, which is available for a direct interaction with the metal surface of the SERS substrate, is much higher than that present in whole plasma. Some of the bands observed can be assigned to specific molecular vibrations of IMT on the basis of the available literature. In particular, according with the *ab initio* theoretical study performed by Srivastava et al.,[46] the SERS band observed at 988 cm^{-1} can be assigned to the R4 (Aminopyrimidine ring) out of plane bending; the band at 1032 cm^{-1} to the stretching and deformation of the R5 (Pyridine ring); the band at 1307 cm^{-1} to the R1 (*N*-methyl piperazine ring) twisting and wagging normal mode and the band at 1609 cm^{-1} to R2 ring deformation.

As mentioned, the SERS bands assigned to IMT are variably downshifted by less than 20 cm^{-1} with respect to the corresponding Raman bands (Figure 2D). Although a detailed description of the molecular adsorption mode from SERS data is nontrivial and it goes beyond the scope of this study, such relatively small differences between SERS and Raman spectra could be tentatively interpreted in favor of a physical adsorption, not involving substantial rearrangements of valence electrons, rather than a chemisorption.[47]

PLSR Model. A PLSR model for IMT quantification in plasma was constructed using a final data matrix consisting of 84 rows (7 spectra for each concentration) and 448 columns (SERS spectra wavelengths). After rdCV validation scheme, 8400 test set predicted values were produced. It must be stressed that all the predicted values are from test sets containing samples not used for model generation/optimization, and are therefore appropriate for a reasonable estimation of the prediction performance. Considering the optimized number of LVs (3, accounting for the 90% of the total spectral data variance), it was possible to ensure that an appropriate number of samples was employed, according to ASTM guidelines,[48] which prescribe an empirical estimation of ten times the number of LVs + 1, among calibration and validation. The PLSR predictions for the IMT concentrations with the estimated individual uncertainty obtained by rdCV are reported in Figure 3A. Model performance is described comparing the predicted IMT concentration versus the actual

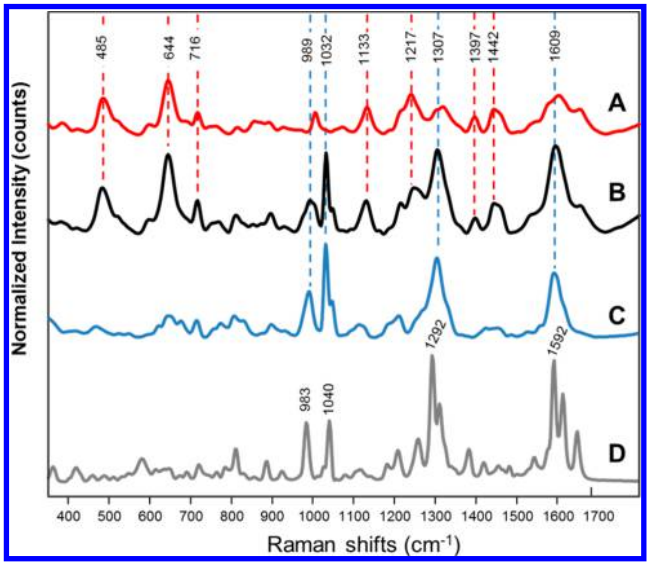

Figure 3. Spectra of imatinib different solutions: (A) deproteinized plasma (no IMT), (B) IMT in plasma, (C) IMT in MeOH/Zn^{2+} solution, and (D) IMT powder.

concentration. The boxes in the plot reflect the distribution of prediction error relatively to the between-models variances in the compound concentration, providing a reliable picture of the predictive performance of the model. The results show a good linearity (R^2 = 0.90), a low prediction error, with an overall SEP of 510 ng/mL, and a negligible bias.

A tolerance interval for the prediction errors is deduced from the distribution of the residuals (Figure S2A), the 2.5% and 97.5% percentiles defining the lower and the upper limits of a 95% confidence interval. Table 1 contains a summary of the statistics for the PLSR model. To better inspect the developed PLS model, regression coefficients are presented in Figures 4B. In spite of their spectrum-like aspect, they are not spectra. The relative size of the coefficients reflects the underlying structure of the data.[49] In this respect, they were used to check the effects of different bands in determination of IMT concentration in plasma. Large positive values indicate the cumulative importance and significance of the effects of that wavenumber for the prediction. According to Figure 4B, we can appreciate a strong contribution from bands ascribable to IMT (988, 1032, 1307, 1609 cm^{-1}), supporting the model capacity to determine the analyte in the presence of interferences from other matrix constituents, if they were included in the calibration phase (this corresponds to the so-called first order advantage).[50] With a similar purpose, it is possible to look at the loadings and loading weights, used in developed PLS model (Figure S5). However, for spectral-like data, no consensus exists on universal rules for interpretation. The main reason to look at loadings (weights) is still to check how noisy they are.[51]

Table 1. Statistical Parameters of PLSR Model[a]

parameter	values
data matrix	
spectra × wavenumbers	84 × 448
LVs	3
SEP_{final} (TI_{95})	
ng/mL	510 (−1056:+839)
μM	1.033 (−2.4:+1.7)
residuals mean (TI_{95})	
ng/mL	10 (13−31)
μM	0.021 (0.027−0.062)
R^2 (TI_{95})	0.90 (0.89−0.92)

[a]LVs, Final number of latent variables; SEP_{final}, standard error of prediction, TI_{95}, 95%-tolerance interval; R^2, squared correlation coefficient.

Analytical Validation. Table 2 summarizes the parameters estimated for evaluating the main FOM of the proposed method. The decision limit (CCα) and the capability of detection (CCβ) were determined from hypothesis test and verification experiment for probabilities of false positive (absence of analyte, α) and false negative (presence of analyte, β) equal to 0.05, so the values achieved were 105 and 210 ng/mL, respectively. This means that for values less than 105 ng/mL, the predicted IMT concentration is noncompliant with a 5% probability that this assertion be false. But in this case the probability β, to assert that a sample has concentration greater than or equal to 105 ng/mL when it is false, is 50% (50% risk

Table 2. Figures of Merit[a]

figure of merit	parameter	values
accuracy	RMSEP	484 ng/mL (0.98 μM)
systematic error	BIAS	133 ng/mL (0.27 μM)
precision	SEP	510 ng/mL (1.033 μM)
	TI_{95}	−1056:+839 ng/mL (−2.14:+1.70 μM)
decision limit	CCα	105 ng/mL (0.22 μM)
limit of detection	CCβ	210 ng/mL (0.43 μM)
limit of quantitation	LOQ	636 ng/mL (1.29 μM)
sensitivity	SEN	8.21×10^{-3} au mL/ng
analytical sensitivity	γ	5.65×10^{-3} mL/ng
inverse of analytical sensitivity	γ^{-1}	178 ng/mL (0.36 μM)

[a]RMSEP, root mean squared error of prediction; BIAS, mean of the prediction errors; SEP, standard error of prediction; TI_{95}, 95%-tolerance interval.

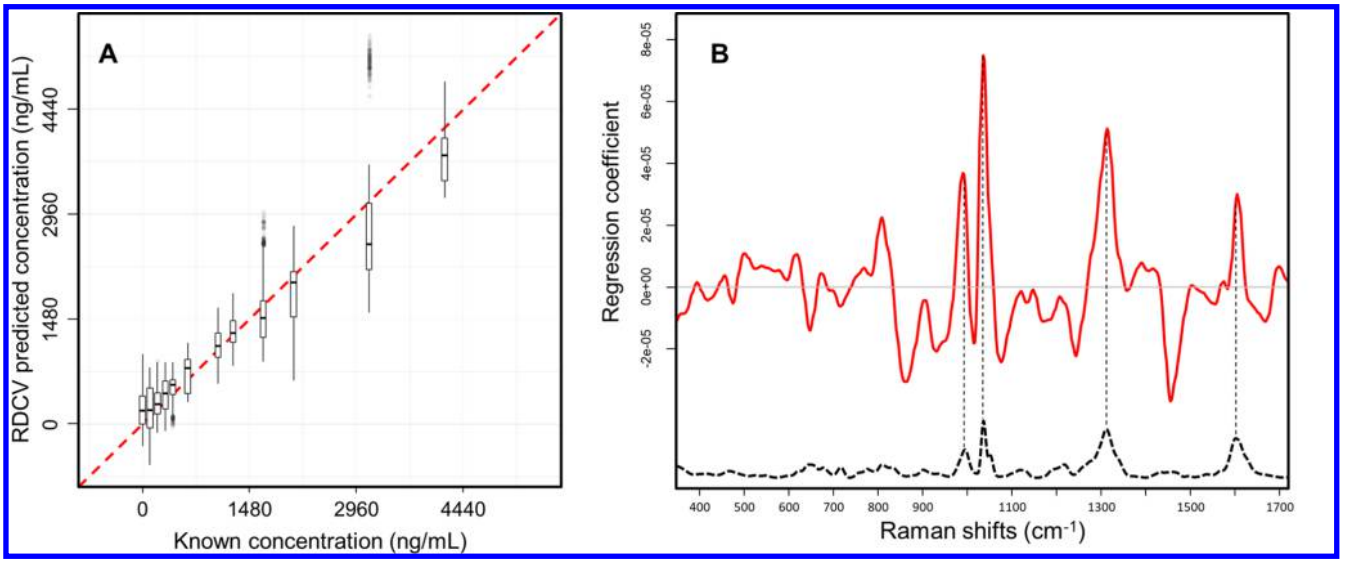

Figure 4. Evaluation of PLSR. A. Actual vs predicted plot. The boxplots reflect the estimated uncertainty associated with individual predictions after 100 repetitions. B. Regression coefficients for the prediction of IMT in plasma using PLSR. SERS spectrum of IMT in MeOH:2% ZnSO4 (dashed black line) is included for comparison: all main structural features are reproduced by the regression model.

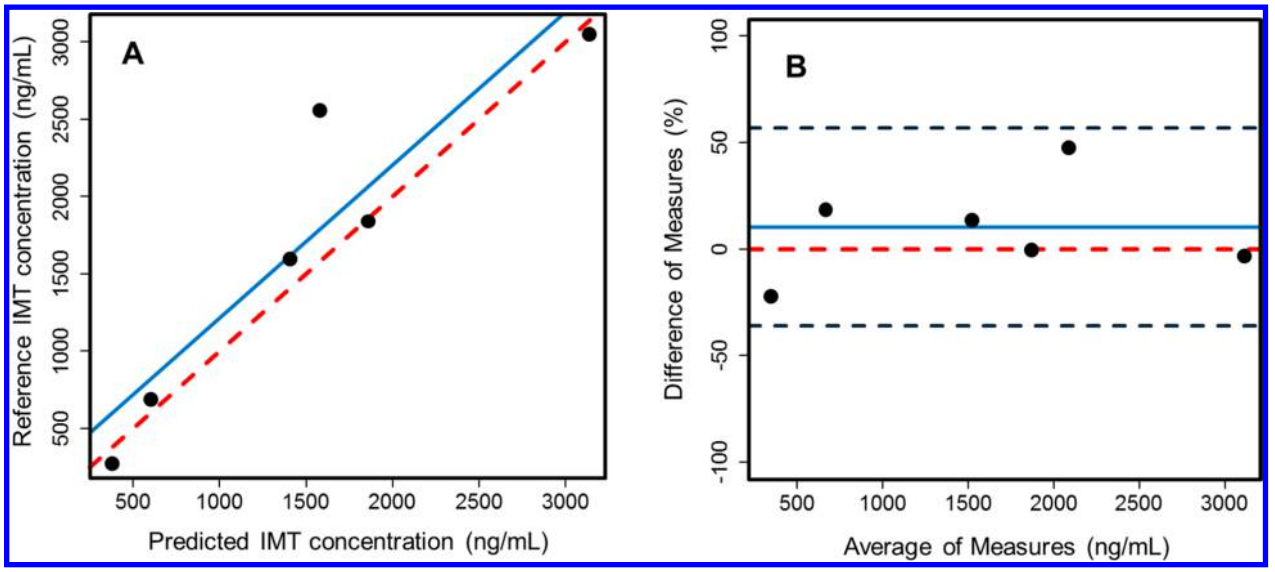

Figure 5. Comparison of IMT C_{trough} plasma concentrations in six real clinical samples. Concentrations were determined with the newly developed SERS method and by an LC−MS/MS method. (A) Predicted vs reference concentration plot. (B) Bland-Altman plot comparison. The red dashed line is the identity line; the solid blue line represents the line of mean bias, with the upper and lower lines indicating the 95% agreement limits.

of false negatives). However, if the PLS model provides a value of 210 ng/mL (equal to CCβ) for test sample, then β is reduced to 5%. The limit of quantitation of the SERS detection (LOQ) was 636 ng/mL. Sensitivity (SEN) was estimated as 8.21×10^{-3} a.u. mL/ng (Table 2). Since this value is dependent on the analytical technique employed and the analyzed matrix, it is not useful for comparison with other methods. Thus, generalized analytical sensitivity (γ) was also calculated as 5.65×10^{-3} mL/ng, based on the obtained estimate of the instrumental noise. The inverse of γ, 178 ng/mL, provides an estimate of the minimum concentration difference that the method can statistically distinguish. Considering the proposed IMT C_{trough} cutoff, approximately round 1100 ng/mL, the application of the SERS method for dosing IMT seems reasonable. To demonstrate the applicability of the SERS method coupled with multivariate calibration to real clinical samples, the developed method was applied to the determination of IMT in samples from six patients at National Cancer Institute (Aviano, Italy), and the results were in good agreement (R^2 = 0.93) with those from HPLC−MS/MS (Figure 5A and Table 3). Accuracy was estimated through the absolute error parameters, such as RMSEP (484 ng/mL) with SEP (510 ng/mL) measuring the precision and BIAS (133 ng/mL) the trueness, respectively. These data demonstrated good accuracy of the SERS method.

Table 3. Imatinib Prediction Results

patient	SERS prediction (ng/mL)	LC−MS/MS reference (ng/mL)
1	3120	3070
2	582	711
3	1387	1616
4	1560	2577
5	360	293
6	1841	1861
R^2	0.93	
mean difference	11%	
SD difference	24%	

As shown by the Bland-Altman plot in Figure 5B, the SERS method had a mean difference of 11% (limits of agreement, ±1.96 SD of mean, from −36% to 57%) for IMT detection compared to the standard method. These limits of agreement depict a partial robustness of the PLS model despite acceptable performance.

However, Bland-Altman plots are influenced by the sample size, and six samples used for method comparison are probably too small to obtain stable results.[52] It must be noted that less than 2 min were required for a spectral acquisition, and spectral prediction of samples was instantaneous. In comparison to chromatographic methods that involve elution with solvents, the SERS method requires few consumables, is faster, and less expensive. Furthermore, it should be pointed out that this technique does not require highly trained personnel to operate it and that the Raman spectrometer used is portable and as such this method could be applied in a point of care setting down the line. However, the results presented in this study, which mainly aimed at assessing the overall feasibility of IMT SERS detection in plasma, and in particular the limits of such an approach in terms of precision are to be carefully considered as promising. Ideally, further studies involving a far greater number of clinical samples should be performed as a definitive validation of the method proposed in this preliminary work.

■ ASSOCIATED CONTENT

Supporting Information

The Supporting Information is available free of charge on the ACS Publications Web site. . The Supporting Information is available free of charge on the ACS Publications website at DOI: 10.1021/acs.analchem.8b02901.

Full experimental details of all FOM calculations; chromatographic and spectrometric conditions of the reference method (Table S1); MRM parameters of the considered analytes (Table S2); spectra before and after preprocessing (Figure S1); SERS spectra of different concentrations of IMT after preprocessing (Figure S2); diagnostic plots for the evaluation of PLS model by

Repeated Double Cross Validation (Figures S3 and S4); comparison of PLS loadings and loading weights for the SERS model (Figure S5); and confidence intervals for the regression coefficients (Figure S6) (PDF)

AUTHOR INFORMATION

Corresponding Author

*E-mail: sfornasaro@units.it.

ORCID

Stefano Fornasaro: 0000-0003-3057-7559

Author Contributions

The manuscript was written through contributions of all authors. All authors have given approval to the final version of the manuscript.

Notes

The authors declare no competing financial interest.

ACKNOWLEDGMENTS

S.F., A.B., E.M., G.T., and V.S. thank Associazione Italiana per la Ricerca sul Cancro (AIRC) for the financial support of this work (Project 12214, Innovative Tools for Cancer Risk Assessment and Early Diagnosis −5 x1000). T.R. and M.S.S. acknowledge the support of the Danish National Research Foundation (Grant DNRF122), and Villum Fonden (Grant No. 9301).

REFERENCES

(1) Widmer, N.; Decosterd, L. A.; Csajka, C.; Leyvraz, S.; Duchosal, M. A.; Rosselet, A.; Rochat, B.; Eap, C. B.; Henry, H.; Biollaz, J.; Buclin, T. *Br. J. Clin. Pharmacol.* **2006**, *62*, 97−112.

(2) Haouala, A.; Widmer, N.; Guidi, M.; Montemurro, M.; Leyvraz, S.; Buclin, T.; Eap, C. B.; Decosterd, L. A.; Csajka, C. *Br. J. Clin. Pharmacol.* **2013**, *75*, 1007−1018.

(3) Petain, A.; Kattygnarath, D.; Azard, J.; Chatelut, E.; Delbaldo, C.; Geoerger, B.; Barrois, M.; Seronie-Vivien, S.; LeCesne, A.; Vassal, G. *Clin. Cancer Res.* **2008**, *14*, 7102−7109.

(4) Gao, B.; Yeap, S.; Clements, A.; Balakrishnar, B.; Wong, M.; Gurney, H. *J. Clin. Oncol.* **2012**, *30*, 4017−4025.

(5) Gotta, V.; Bouchet, S.; Widmer, N.; Schuld, P.; Decosterd, L. A.; Buclin, T.; Mahon, F. X.; Csajka, C.; Molimard, M. *Leuk. Res.* **2014**, *38*, 764−772.

(6) von Mehren, M.; Widmer, N. *Cancer Treat. Rev.* **2011**, *37*, 291−299.

(7) Verheijen, R. B.; Yu, H.; Schellens, J. H. M.; Beijnen, J. H.; Steeghs, N.; Huitema, A. D. R. *Clin. Pharmacol. Ther.* **2017**, *102*, 765−776.

(8) Widmer, N.; Bardin, C.; Chatelut, E.; Paci, A.; Beijnen, J.; Leveque, D.; Veal, G.; Astier, A. *Eur. J. Cancer* **2014**, *50*, 2020−2036.

(9) Haouala, A.; Zanolari, B.; Rochat, B.; Montemurro, M.; Zaman, K.; Duchosal, M. A.; Ris, H. B.; Leyvraz, S.; Widmer, N.; Decosterd, L. A. *J. Chromatogr. B: Anal. Technol. Biomed. Life Sci.* **2009**, *877*, 1982−1996.

(10) Bouchet, S.; Chauzit, E.; Ducint, D.; Castaing, N.; Canal-Raffin, M.; Moore, N.; Titier, K.; Molimard, M. *Clin. Chim. Acta* **2011**, *412*, 1060−1067.

(11) Widmer, N.; Beguin, A.; Rochat, B.; Buclin, T.; Kovacsovics, T.; Duchosal, M. A.; Leyvraz, S.; Rosselet, A.; Biollaz, J.; Decosterd, L. A. *J. Chromatogr. B: Anal. Technol. Biomed. Life Sci.* **2004**, *803*, 285−292.

(12) McKeating, K. S.; Aubé, A.; Masson, J.-F. *Analyst* **2016**, *141*, 429−449.

(13) Jaworska, A.; Fornasaro, S.; Sergo, V.; Bonifacio, A. *Biosensors* **2016**, *6*, 47.

(14) Rath, S.; Sahu, A.; Gota, V.; Martínez-Torres, P. G.; Pichardo-Molina, J. L.; Murali, K. *J. Innovative Opt. Health Sci.* **2015**, *8*, 1550019.

(15) Shah, V. P.; Midha, K. K.; Findlay, J. W.; Hill, H. M.; Hulse, J. D.; McGilveray, I. J.; McKay, G.; Miller, K. J.; Patnaik, R. N.; Powell, M. L.; Tonelli, A.; Viswanathan, C. T.; Yacobi, A. *Pharm. Res.* **2000**, *17*, 1551−1557.

(16) Oostendorp, R. L.; Beijnen, J. H.; Schellens, J. H.; Tellingen, O. *Biomed. Chromatogr.* **2007**, *21*, 747−754.

(17) Yang, L.; Liu, H.; Ma, Y.; Liu, J. *Analyst* **2012**, *137*, 1547−1549.

(18) Yang, L.; Li, P.; Liu, H.; Tang, X.; Liu, J. *Chem. Soc. Rev.* **2015**, *44*, 2837−2848.

(19) Beleites, C.; Sergo, V. *hyperSpec: a package to handle hyperspectral data sets in R*, R package version 0.99-20171005 2017.

(20) Filzmoser, P.; Varmuza, K. *chemometrics: Multivariate Statistical Analysis in Chemometrics*, R package version 1.4.2 2017.

(21) Liland, K. H. *EMSC: Extended Multiplicative Signal Correction*, R package version 0.8.2 2017.

(22) Mevik, B.-H.; Wehrens, R. *Journal of Statistical Software* **2007**, *18*, 1−23, DOI: 10.18637/jss.v018.i02.

(23) Aphalo, P. J. *UV4Plants Bulletin* **2015**, *2015*, 21−29.

(24) Kohler, A.; Kristian Afseth, N.; Martens, H. In *Applications of Vibrational Spectroscopy in Food Science*; Li-Chan, E. C. Y., Chalmers, J. M., Griffiths, P. R., Eds.; John Wiley & Sons, 2010.

(25) Afseth, N. K.; Kohler, A. *Chemom. Intell. Lab. Syst.* **2012**, *117*, 92−99.

(26) Liland, K. H.; Kohler, A.; Afseth, N. K. *J. Raman Spectrosc.* **2016**, *47*, 643−650.

(27) Wold, S.; Sjöström, M.; Eriksson, L. *Chemom. Intell. Lab. Syst.* **2001**, *58*, 109−130.

(28) Martens, H.; Naes, T. *Multivariate Calibration*; John Wiley & Sons, 1992; p 444.

(29) Filzmoser, P.; Liebmann, B.; Varmuza, K. *J. Chemom.* **2009**, *23*, 160−171.

(30) Hastie, T.; Tibshirani, R.; Friedman, J. H. *The Elements of Statistical Learning: Data Mining, Inference, And Prediction*, 2nd ed.; Springer: New York, 2009; p xxii, 745 pages.

(31) Magnusson, B.; Örnemark, U. *Eurachem Guide: The Fitness for Purpose of Analytical Methods − A Laboratory Guide to Method Validation and Related Topics*, 2nd ed.; Eurachem, 2014.

(32) Olivieri, A. C. *Anal. Chim. Acta* **2015**, *868*, 10−22.

(33) Fragoso, W.; Allegrini, F.; Olivieri, A. C. *Anal. Chim. Acta* **2016**, *933*, 43−49.

(34) Allegrini, F.; Wentzell, P. D.; Olivieri, A. C. *Anal. Chim. Acta* **2016**, *903*, 51−60.

(35) Ortiz, M. C.; Sarabia, L. A.; Sanchez, M. S. *Anal. Chim. Acta* **2010**, *674*, 123−142.

(36) Feinberg, M. *J. Chromatogr A* **2007**, *1158*, 174−183.

(37) Bland, J. M.; Altman, D. G. *Lancet* **1986**, *327*, 307−310.

(38) Dalla Marta, S.; Novara, C.; Giorgis, F.; Bonifacio, A.; Sergo, V. *Materials* **2017**, *10*, 1365.

(39) Fornasaro, S.; Dalla Marta, S.; Rabusin, M.; Bonifacio, A.; Sergo, V. *Faraday Discuss.* **2016**, *187*, 485−499.

(40) Wu, K.; Rindzevicius, T.; Schmidt, M. S.; Mogensen, K. B.; Hakonen, A.; Boisen, A. *J. Phys. Chem. C* **2015**, *119*, 2053−2062.

(41) Schmidt, M. S.; Hübner, J.; Boisen, A. *Adv. Mater.* **2012**, *24*, OP11−OP18.

(42) Polson, C.; Sarkar, P.; Incledon, B.; Raguvaran, V.; Grant, R. *J. Chromatogr. B: Anal. Technol. Biomed. Life Sci.* **2003**, *785*, 263−275.

(43) Shokati, T.; Bodenberger, N.; Gadpaille, H.; Schniedewind, B.; Vinks, A. A.; Jiang, W.; Alloway, R. R.; Christians, U. *J. Visualized Exp.* **2015**, e52424.

(44) Bonifacio, A.; Dalla Marta, S.; Spizzo, R.; Cervo, S.; Steffan, A.; Colombatti, A.; Sergo, V. *Anal. Bioanal. Chem.* **2014**, *406*, 2355−2365.

(45) Premasiri, W. R.; Lee, J. C.; Ziegler, L. D. *J. Phys. Chem. B* **2012**, *116*, 9376−9386.

(46) Srivastava, A.; Joshi, B. D.; Tandon, P.; Ayala, A. P.; Bansal, A. K.; Grillo, D. *Spectrochim. Acta, Part A* **2013**, *103*, 325−332.

(47) Aroca, R. *Surface Enhanced Vibrational Spectroscopy*; Wiley ; Chichester, U.K., 2006.

(48) *Standard Guide for Validating Analytical Methods*; ASTM International: West Conshohocken, PA, 2016.
(49) Burnham, A. J.; MacGregor, J. F.; Viveros, R. *J. Chemom.* **2001**, *15*, 265−284.
(50) Olivieri, A. C. *Anal. Chem.* **2008**, *80*, 5713−5720.
(51) Fearn, T. *NIR news* **2003**, *14*, 8−9.
(52) Stockl, D.; Rodriguez Cabaleiro, D.; Van Uytfanghe, K.; Thienpont, L. M. *Clin. Chem.* **2004**, *50*, 2216−2218.